The Journal of Infectious Diseases

MAJOR ARTICLE

Evaluating Treatment Efficacy in a Mouse Model of Enterovirus D68–Associated Paralytic Myelitis

Alison M. Hixon,[1,2] Penny Clarke,[3] and Kenneth L. Tyler[3,4,5]

[1]Medical Scientist Training Program, [2]Neuroscience Program, [3]Department of Neurology, [4]Department of Medicine, and [5]Department of Immunology and Microbiology, University of Colorado School of Medicine, Aurora

Background. Enterovirus D68 (EV-D68)–associated acute flaccid myelitis (AFM) is a devastating neurological disease for which there are no treatments of proven efficacy. The unpredictable temporal and geographic distribution of cases and the rarity of the disease make it unlikely that data from randomized controlled trials will be available to guide therapeutic decisions. We evaluated the following 3 widely used empirical therapies for the ability to reduce the severity of paralysis in a mouse model of EV-D68 infection: (1) human intravenous immunoglobulin (hIVIG), (2) fluoxetine, and (3) dexamethasone.

Methods. Neonatal mice were injected intramuscularly with a human 2014 EV-D68 isolate that reliably induces paralysis in mice due to infection and loss of spinal cord motor neurons. Mice receiving treatments were evaluated for motor impairment, mortality, and spinal cord viral load.

Results. hIVIG, which contained neutralizing antibodies to EV-D68, reduced paralysis in infected mice and decreased spinal cord viral loads. Fluoxetine had no effect on motor impairment or viral loads. Dexamethasone treatment worsened motor impairment, increased mortality, and increased viral loads.

Conclusion. Results in this model of EV-D68–associated AFM provide a rational basis for selecting empirical therapy in humans and establish this model as a useful system for evaluating other potential therapies.

Keywords. Enterovirus D68; acute flaccid myelitis; paralysis; therapies; mouse model.

Enterovirus D68 (EV-D6) is a member of the Enterovirus genus, which includes polioviruses, but it is primarily a respiratory pathogen, with features more similar to rhinoviruses [1, 2]. EV-D68 was first isolated in 1962 from children in California with respiratory illnesses but, until recently, was only rarely documented to be a cause of human disease [3–5]. In the last decade, EV-D68 became an emerging pathogen responsible for outbreaks of respiratory disease worldwide [6, 7]. During 2014, EV-D68 caused an outbreak of respiratory disease in the United States that was associated with 120 confirmed cases of a polio-like paralytic condition called acute flaccid myelitis (AFM), primarily in children [8–18]. AFM presents as sudden onset of limb weakness with or without cranial nerve involvement, with associated magnetic resonance imaging (MRI) findings of a longitudinally extensive multisegmental myelitis predominantly involving the anterior spinal cord [19]. Neurological examination and electromyogram and nerve conduction studies are consistent with lower motor neuron damage [12, 16, 19, 20]. While polioviruses and other nonpoliovirus enteroviruses are recognized causes of AFM, this was the first time that EV-D68 had been widely associated with the condition. Another 144 confirmed cases of EV-D68–associated AFM occurred in the United States in 2016 [18, 21–23], and additional cases have been reported all over the world [24–32].

Current treatment of AFM is empirical. Commonly used modalities include agents directed at reducing immune responses and inflammation, such as plasmapheresis and high-dose corticosteroids. Another widely used therapy, human intravenous immunoglobulin (hIVIG), potentially has both immunomodulatory and antiviral properties. Most patients with AFM have been treated with multiple agents, making assessment of the efficacy, if any, of individual agents problematic [12, 16]. Regardless of the intervention, the prognosis of AFM is poor, with most patients having residual functional deficits and only a minority of patients fully recovering [12, 16, 33].

Screening and evaluation of potential treatments for EV-D68–associated AFM has been facilitated by the recent development of a neonatal mouse model that replicates the cardinal features of the human disease [34]. Specific EV-D68 strains from the 2014 outbreak inoculated into neonatal mice produce paralysis resulting from infection and subsequent death of spinal cord motor neurons [34]. The current study uses this EV-D68 murine model to investigate the clinical efficacy of 3 treatment modalities commonly used in cases of human AFM, including hIVIG, high-dose corticosteroids (dexamethasone), and fluoxetine.

Received 3 August 2017; editorial decision 30 August 2017; accepted 7 September 2017; published online September 13, 2017.

Presented in part: 14th International Symposium on Neurovirology, Toronto, Canada, 25–28 October 2016; 69th Annual Meeting of the American Academy of Neurology, Boston, Massachusetts, 22–28 April 2017.

Correspondence: K. L. Tyler, Department of Neurology, University of Colorado School of Medicine, Research Complex 2, Mail Stop B-182, 12700 E 19th Ave, Aurora, CO 80045 (ken.tyler@ucdenver.edu).

DOI: 10.1093/infdis/jix468

Fluoxetine (Prozac) is a Food and Drug Administration (FDA)–approved antidepressant that has been shown to reduce EV-D68 growth in cell culture through mechanisms independent of its antidepressant mode of action (inhibition of serotonin reuptake) [35, 36] and has recently been used in the treatment of AFM [37, 38].

METHODS

Viral Stocks

Representative strains IL/14-18952 (clade B), MO/14-18947 (clade B1), and KY/14-18953 (clade C) from clades circulating during the 2014 EV-D68 respiratory outbreak were obtained from the BEI Resources Repository, an infectious diseases research specimen repository (managed under the American Type Culture Collection [ATCC]). Fermon, an ancestral EV-D68 strain isolated in 1962, was obtained courtesy of Dr Shigeo Yagi at the California Department of Public Health and was used as a control. Viral stocks were grown in rhabdomyosarcoma (RD) cells (ATCC) at 33°C and 5% CO_2 until most cells were dead or dying. Cells debris was removed from RD cell–grown stocks by ultracentrifugation. Titers of viral stocks were determined by a 50% tissue culture infectious dose ($TCID_{50}$) assay as calculated by the Kärber method.

Mouse Experiments

All studies were done in accordance with the University of Colorado Institutional Animal Care and Use Committee regulations in an AAALAC International–accredited facility under an approved protocol. Two-day-old National Institutes of Health Swiss Webster mouse pups of both sexes were used for all experiments unless otherwise noted. Animals were maintained in biosafety level 2 housing conditions following infection. Mouse pups were weighed and monitored daily for signs of disease across all experiments. Mice that appeared unable to nurse (ie, those that lacked milk in their stomach), exhibited failure to thrive (ie, those that consistently lost weight), or became immobile (those that were lying on their side and unable to self-propel) were euthanized to minimize suffering. Across all motor scoring experiments, treatment groups consisted of 1 litter of mice (8–12 pups) that were always compared to a control litter of mice born the same day. To minimize variability between these groups, mice from the 2 litters were randomly sorted into either the experimental or control groups before virus injection. All motor scoring was done by individuals blinded to treatment group. For all viral titer analysis experiments, 2–4 litters of mice were compared per experiment.

Virus Injections

EVD-68 isolate IL/14-18952 was injected (10 µL) into the medial thigh muscles of the left hind limb of 2-day-old pups. Uninfected control mice received a similar inoculation of RD cell media processed in the same manner as viral stocks. The viral titers that were used are noted in the individual experiments.

Intravenous Immunoglobulin

Gamunex-C 10% hIVIG was obtained from Children's Hospital Colorado (lot P1GD600201; Grifols). On day 1, 3, 4, or 6 after infection, mouse pups were administered 100 µL of IVIG by intraperitoneal injection or 100 µL of sterile phosphate-buffered saline (PBS; pH 7.4) as an injection control.

Fluoxetine Injections

Fluoxetine hydrochloride was obtained as a powder from Sigma Aldrich (catalog no. F132), with all stocks made fresh in PBS on the day of inoculation. Starting on day 0 after infection, mice received either fluoxetine by intraperitoneal injection or an equivalent volume of sterile PBS control. Treatment was given for 7 days, from 0 to 6 days after infection. For viral tissue titer comparison experiments, mice were euthanized on day 6 after infection, several hours after administration of the final dose of fluoxetine.

Dexamethasone Injections

Dexamethasone was obtained as a powder from Sigma Aldrich (catalog no. D1756). On the day of the experiment, a working stock of 0.1 mg/mL in sterile PBS was prepared. On days 3 and 4 (early treatment) or days 6 and 7 (late treatment) after infection, mouse pups were administered 100 µL of dexamethasone by intraperitoneal injection or 100 µL of sterile PBS control.

Viral Titer Analyses

Mouse pups were decapitated, and the spinal column was transected at the level of the sacrum. Spinal cords were extruded from the spinal column by applying a jet of sterile saline into the spinal canal at the dorsal transection, resulting in ejection of the cord en bloc through the ventral opening. Muscle tissue specimens were collected from the inoculated left leg. Tissue specimens were placed into preweighed BeadBug Tubes containing 0.3 mL of ice-cold, sterile PBS and weighed. BeadBug tubes were then shaken 2 times for 45 seconds at 2000 rpm on a BeadBug tissue homogenizer to lyse the tissue. Samples were frozen at −80°C before use. The viral titer was determined in all tissue lysates by a $TCID_{50}$ assay. Before plating, tubes were spun at 2700 × g (rotor size 9.5 cm) rpm for 1 minute in order to remove tissue from the lysate. Lysates were serially diluted 10-fold and plated from 1 (raw lysate) to $1{:}10^{-6}$. The final titer was determined by the Kärber method.

Mouse Serum Collection

Mice were inoculated by intramuscular injection with 10^3 $TCID_{50}$ of EV-D68 strain IL/14-18952 (n = 10) or control medium (n = 6). On day 21 after infection, mice were anesthetized with isoflurane, and blood specimens were collected by cardiac puncture. Whole-blood specimens were centrifuged at

20 800 x g (rotor size 9.5 cm) for 10 minutes at 4°C to separate cell and serum fractions. Serum from individuals in each group was pooled and frozen at −20°C.

Antibody Neutralization Assay

hIVIG or mouse serum was diluted 1:10 in standard medium (Dulbecco's minimal essential medium containing 10% fetal bovine serum) and then serially diluted 2-fold from 1:10 to 1:20 480. Serum was heat activated for 30 minutes at 56°C before serial dilution. Stock virus (IL/14-18952, US/MO/14-18947, KY/14-18953, or Fermon) at a concentration of 100 $TCID_{50}$ and was mixed at a ratio of 1:1 with serial dilutions of hIVIG or serum and incubated for 1 hour at 37°C. After incubation, the mixture was inoculated into appropriate wells of 96-cell plates containing subconfluent RD cells, and the entire plate was placed in an incubator with a temperature of 33°C and 5% CO_2. Cells were observed for evidence of cytopathic effect for 2 weeks. Diluent and hIVIG or serum were mixed at a ratio of 1:1 and used as a negative control; diluent and virus were mixed at a ratio of 1:1 as a positive control. The neutralization titer was estimated by the Spearman-Kärber method from 3 separate trials with each dilution performed in triplicate. Neutralizing titers were graphed as the inverse of the dilution expressed in $\log_2$ form.

Statistics

Statistical analyses were done using GraphPad Prism, version 7 (Carlsbad, CA). Drug treatment groups were compared using 2-way analysis of variance (ANOVA) for treatment condition and time, followed by the Dunnett multiple comparisons test, to investigate whether there was a main effect of treatment condition. Because each experimental group was compared to a control group, there were multiple control groups per drug treatment. Control groups were pooled after ANOVA, followed by the Dunnett multiple comparisons test, showed no statistical differences between them. Viral titers in muscle or spinal cord tissue specimens were compared between experimental and control groups by using an unpaired Student *t* test. If variance differed significantly between groups as assessed by an F test for variance, groups were instead compared by the Welch *t* test. Survival curves of treatment were compared by the Gehan-Breslow-Wilcoxon test. For all experiments, probability value differences were considered significant at a *P* value of ≤.05.

RESULTS

Intramuscular EV-D68 Injection Model for Quantifying Motor Outcomes

We have previously shown that 2014 EV-D68 strains can efficiently produce paralysis in neonatal mice following intramuscular injection. Mice inoculated intramuscularly with a high dose of paralytogenic EV-D68 can have an onset of paralysis within 3–5 days of viral inoculation [34]. Viral genome, viral antigen, and infectious virus are consistently found in the spinal cords of these animals [34].

To quantify the development of motor impairments in mice receiving intramuscular EV-D68, separate groups of mice received injections of increasing doses of paralytogenic EV-D68 strain IL/14-18952 into their left hind limb on postnatal day 2. Motor impairment was assessed using a previously validated scoring system modified for use in neonatal mice (Table 1) [39]. The higher the motor impairment scores, the worse the motor impairment and experimental outcome.

Mice developed progressively more severe motor impairment in a virus dose–dependent fashion (Figure 1A). A total of 10^4 $TCID_{50}$ of virus significantly increased mortality, with surviving mice having similar scores seen at 10^3 $TCID_{50}$ (Figure 1A). Signs of paralysis always proceeded in a stereotypical pattern, beginning with the injected limb, followed by the contralateral hind limb. Only following hind limb paralysis did some animals develop paralysis in their forelimbs. As the injected viral doses increase, onset occurred earlier and progression of motor impairments was faster (Figure 1A). Mice that died before the experimental end point had more severe motor impairment with higher motor impairment scores (ie, paralysis in hind limbs and forelimbs) than those that survived. These data are summarized in Table 2.

A total of 10^3 $TCID_{50}$ was chosen as a challenge dose for subsequent treatment experiments because it resulted in consistent bilateral rear limb paralysis in the majority of mice, with minimal mortality. Following challenge with this dose, virus became detectable in the spinal cord between 2 and 4 days after infection, peaked between 4 and 6 days after infection, and then fell to undetectable levels by 12 days after infection (Figure 1B). Muscle titer rose rapidly within 2 days following injection and peaked just before the rise in spinal cord titer. The muscle titer then began to fall steadily between days 4 and 12 after infection, declining to nearly undetectable levels by day 12 after infection.

hIVIG Improves Motor Outcomes

Recent lots of hIVIG have been found to contain high levels of neutralizing antibodies to EV-D68 [40]. Consistent with this finding, Gamunex-C IVIG (lot P1GD600201) collected from June 2015 to January 2016 from adult human donors contained

Table 1. Motor Impairment Scoring

Score	Description[a]
0	No impairment
1	Mild impairment, ataxia or decreased movement present, toe/knuckle walking
2	Moderate impairment, profound ataxia, limited movement of limb
3	Severe impairment, no movement of limb, limb is non–weight bearing

[a]Mice were observed on a flat surface for several minutes. The final score for each mouse was calculated by adding the scores for each limb.

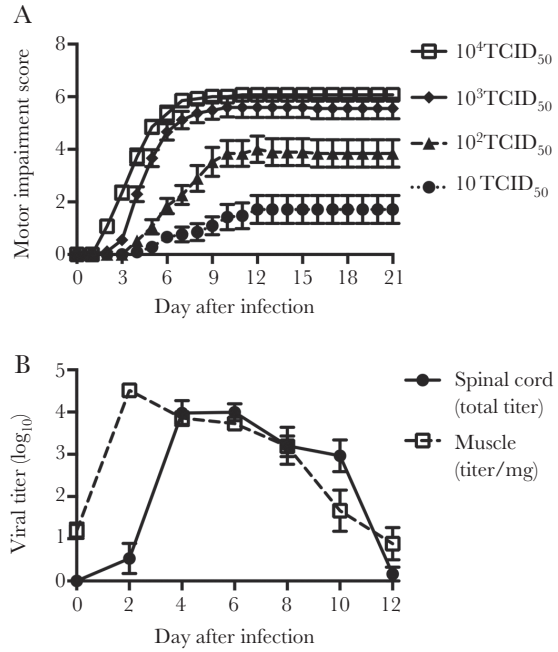

Figure 1. Intramuscular enterovirus D68 (EV-D68) injection model for tracking paralytic disease over time. *A*, Dose response curve for mice given 10 (n = 21), 10^2 (n = 19), 10^3 (n = 27), and 10^4 (n = 14) 50% tissue culture infectious doses (TCID$_{50}$) of EV-D68 IL/14-18952 by intramuscular inoculation, as quantified by motor impairment score for mice surviving to the experimental end point 21 days after infection. *B*, Viral growth in muscle and spinal cord tissue specimens following intramuscular injection with 10^3 TCID$_{50}$ of EV-D68 IL/14-18952 (n = 10 per time point). Error bars are standard errors of the mean.

high levels of neutralizing antibodies to 3 representative EV-D68 strains circulating during the 2014 outbreak—IL/14-18952, MO/14-18947, and KY/14-18953—and to the EV-D68 Fermon strain (Figure 2A). As a comparison, serum from mice inoculated intramuscularly with IL/14-18952 contained similarly high levels of neutralizing antibodies to the infecting IL/14-18952 strain and also neutralized the MO/14-18947 strain, although to a lesser degree (Figure 2B). The antibodies were only minimally neutralizing to EV-D68 strain Fermon, and they failed to neutralize EV-D68 strain KY/14-18953 at any dilution tested (Figure 2B). The serum neutralizing titers in these mice paralleled the phylogenetic relationship of the tested strains. IL/14-18952 and MO/14-18947 belong to closely related EV-D68 genetic clades B and B1, respectively, while KY-18953 belongs to the more distantly related clade A. Fermon is considered an ancestral strain to all modern EV-D68 strains [4]. Serum from uninfected control mice failed to neutralize any strain of EV-D68 at any dilution tested (data not shown).

In this study, mice were given Gamunex-C hIVIG (lot P1GD600201) at increasingly later time points (ie, days 1, 3, 4, and 6 after infection) following inoculation of EV-D68 IL/14-18952. Mice receiving hIVIG on day 1 after infection by intraperitoneal injection did not develop any signs of motor impairment (Figure 3A). Mice given hIVIG on day 3 after infection, a time point coincident with the initial onset of paralysis, developed motor impairment, but it was significantly less severe than that developed by infected control mice (Figure 3A). Mice receiving hIVIG on days 4 or 6 after infection also had significantly lower average motor impairment scores as compared to infected controls. Overall, hIVIG had reduced efficacy the later it was administered in the course of the disease (Figure 3A). Mortality in all groups receiving hIVIG was 0%, while control mortality was 7%. The highest mouse pup weight on day 6 after infection was 6.3 g, and the lowest mouse pup weight on day 1 after infection was 2.1 g. Therefore, the dose of hIVIG was between 1.6 and 4.8 g/kg, varying on the basis of the weight of individual mice across these experimental groups.

To investigate the mechanism by which IVIG reduces signs of paralysis, mice given hIVIG on day 3 following infection were euthanized for viral titer analysis on day 6 after infection. Mice treated with hIVIG had significantly lower viral titers in both spinal cord and muscle tissue specimens, compared with controls (Figure 3B and 3C).

Fluoxetine Has No Effect on Motor Outcomes

Fluoxetine is an FDA-approved serotonin reuptake inhibitor (SSRI) that has been shown to reduce EV-D68 growth in vitro, potentially by inhibition effects on the enteroviral 2C protein [35, 36]. The minimum inhibitory concentration for fluoxetine against EV-D68 has been found to be 0.3–1.05 μM [35]. Mice treated for 7 days with 0.75 mg/kg/day of fluoxetine by intraperitoneal injection starting on the same day as challenge with EV-D68 IL/14-18952 had motor scores identical to those of infected mice treated with vehicle (Figure 4A). Mice treated with 1.5 mg/kg/day of fluoxetine for 7 days and those treated with 3.0 mg/kg/day

Table 2. Summary of Dose-Response Data From an Intramuscular Injection Model

Virus Dose, TCID$_{50}$	Time to Onset of Motor Deficits Among Survivors After Infection, d Range	Motor Score Among Survivors 21 d After Infection, Mean ± SEM	Mortality, %	Motor Score Among Nonsurvivors, Mean ± SEM
10^4	2–3	6.1 ± 0.1	33	9.6 ± 0.4
10^3	2–5	5.6 ± 0.4	18	9.2 ± 0.3
10^2	3–7	3.8 ± 0.5	5	11.0 ± 0
10	4–9	1.7 ± 0.5	0	NA

Abbreviations: NA, not applicable; SEM, standard error of the mean; TCID$_{50}$, 50% tissue culture infectious dose.

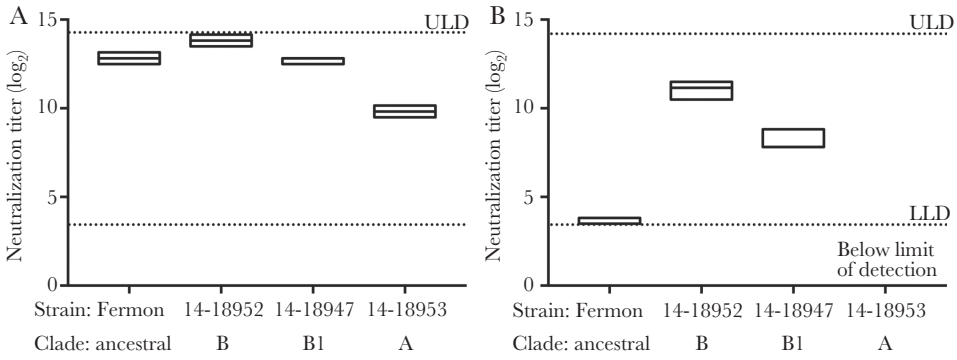

Figure 2. Enterovirus D68 (EV-D68) neutralizing antibody titer in human intravenous immunoglobulin (hIVIG) versus immune mouse serum. *A*, Neutralizing antibody titers of hIVIG used for in vivo experiments against select EV-D68 strains, including the ancestral EV-D68 strain Fermon and three 2014 strains of EV-D68 from different clades: MO/14-18947 (clade B1), IL/14-19852 (clade B), and KY/14-18953 (clade A). *B*, Neutralizing antibody titers in immune serum from mice inoculated with intramuscular EV-D68 IL/14-18952 against the infecting strain IL/14-18952, the closely related strain MO/14-18947, and the more distantly related KY/14-18953 and Fermon strains. Boxes represent 95% confidence intervals with a line at the median. LLD, lower limit of detection; ULD, upper limit of detection.

of fluoxetine for 7 days also failed to show any difference from infected controls (Figure 4A). Mortality was higher in animals receiving fluoxetine as compared to controls (28% vs 6%).

Viral titers in muscle and spinal cord tissue specimens in mice treated with 3.0 mg/kg fluoxetine for 7 days were not significantly different from those in control mice (Figure 4B and 4C), indicating that fluoxetine does not reduce viral load even at the maximal dose tested.

High-Dose Corticosteroids Worsens Mortality and Motor Outcomes

Inflammation can contribute to central nervous system (CNS) damage during infection, but it is unclear how much inflammation versus infection of neurons contributes to neuronal injury and paralysis in EV-D68 experimental myelitis. Intravenous steroids have been used to reduce CNS inflammation, including that in patients with AFM [12, 16]. Here, dexamethasone was administered by intraperitoneal injection on either days 3 and

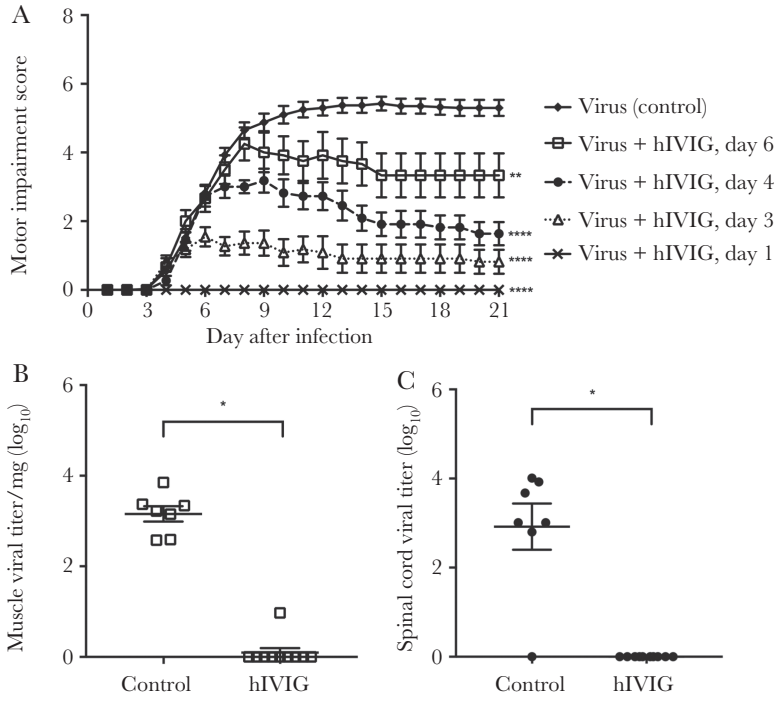

Figure 3. Human intravenous immunoglobulin (hIVIG) reduces enterovirus D68 (EV-D68)–induced motor impairment and viral loads. *A*, Motor impairment scores for mice infected by intramuscular inoculation with 10^3 EV-D68 IL/14-18952 and then given hIVIG by intraperitoneal injection at either 1 day (n = 8), 3 days (n = 11), 4 days (n = 11), or 6 days (n = 12) after infection. Control mice received an intraperitoneal injection of phosphate-buffered saline (n = 40). Data for animals surviving to the end of the study were graphed. *B* and *C*, Mice were treated with hIVIG (n = 10) or control (n = 7) on day 3 after infection. On day 6 after infection, muscle (open squares) and spinal cord (filled circles) tissue specimens were collected for viral titer analysis. Error bars are standard errors of the mean. $*P \le .05$, $**P \le .01$, and $****P \le .0001$.

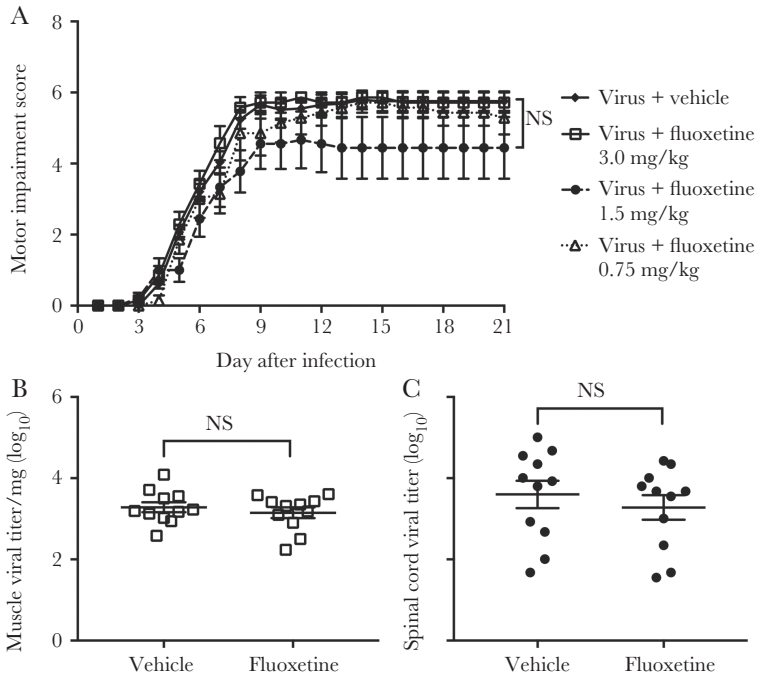

Figure 4. Fluoxetine has no effect on enterovirus D68 (EV-D68)–induced motor impairment and viral loads. *A*, Motor impairment scores for mice infected by intramuscular injection with 10^3 50% tissue culture infectious doses ($TCID_{50}$) of EV-D68 IL/14-18952 and then given fluoxetine by intraperitoneal injection for 7 days on days 0–6 after infection at 3 different concentrations (0.75 mg/kg [n = 7], 1.5 mg/kg [n = 9], or 3.0 mg/kg [n = 7]) versus vehicle control (n = 29). Treatment started the same day as viral infection, defined as day 0 after infection, and ended on day 6 after infection. Data for animals surviving to the end of the study were graphed. *B* and *C*, Mice were treated with 3.0 mg/kg fluoxetine (n = 11) for 7 days (days 0–6 after infection) or vehicle (n = 11) following intramuscular injection of 10^3 $TCID_{50}$ EV-D68 IL/14-18952. On day 6 after infection, several hours after the final dose of fluoxetine, muscle (open squares) and spinal cord (filled circles) tissue specimens were collected for viral titer analysis. Error bars are standard errors of the mean. NS, not significant.

4 (early) or days 6 and 7 (late) after inoculation with EV-D68 IL/14-18952. Daily doses of dexamethasone were 1.7–3.2 mg/kg/d, varying on the basis of the weight of individual mice across these experimental groups. Mice receiving both virus and dexamethasone at either early or late time points had significantly higher mortality as compared to infected controls (Figure 5A). Administration of dexamethasone to uninfected mice did not cause death (Figure 5A). Individual dexamethasone-treated mice that died before the experimental end point had worse paralysis than that associated with the average motor impairment score in infected controls (Figure 5B).

Viral titer in muscle and spinal cord tissue specimens was analyzed for mice surviving on day 6 after infection that received dexamethasone on days 3 and 4 after infection. Dexamethasone resulted in significantly higher titers in spinal cord tissue specimens, compared with controls (Figure 5C), but titers in muscle tissue specimens were not significantly different between treatment groups (Figure 5D).

DISCUSSION

There are currently no therapies of proven efficacy for EV-D68–associated AFM. Randomized control trials of candidate treatments for this disease will be difficult because of its rarity and the geographic and temporal unpredictability of cases. The use of appropriate in vitro and in vivo models can facilitate rational design of empirical therapy. Development of a neonatal mouse model of EV-D68–induced paralysis has facilitated the testing of potential treatments for AFM. Injection of neuroinvasive and neurovirulent EV-D68 into the muscle of neonatal mice produces paralysis that can be tracked and quantified. We used the 2014 EV-D68 strain IL/14-18952 because this produces a reliable and dose-dependent severity of motor paralysis in neonatal mice after intramuscular injection. We chose 10^3 $TCID_{50}$ as a standard dose for challenge experiments because this consistently induced bilateral hind limb paralysis in the majority of mice tested, with only low levels of mortality. The viral titer within spinal cord and muscle tissue specimens from mice receiving 10^3 $TCID_{50}$ EV-D68 IL/14-18952 was quantified over time. Spinal cord titers rose after viral growth in the muscle tissue specimens, suggesting direct spread from infected muscle through motor nerve fibers into the CNS, as has been documented in mouse models of poliomyelitis [41]. Growth of virus in the spinal cord corresponds to the development of motor impairment, indicating that infection is the primary cause of paralysis. The pattern of limb paralysis in the CNS also suggests neuron-to-neuron spread, as virus moves from the motor neurons of the inoculated limb, to the contralateral hind limb, and then, in some mice, to the forelimbs. This model is

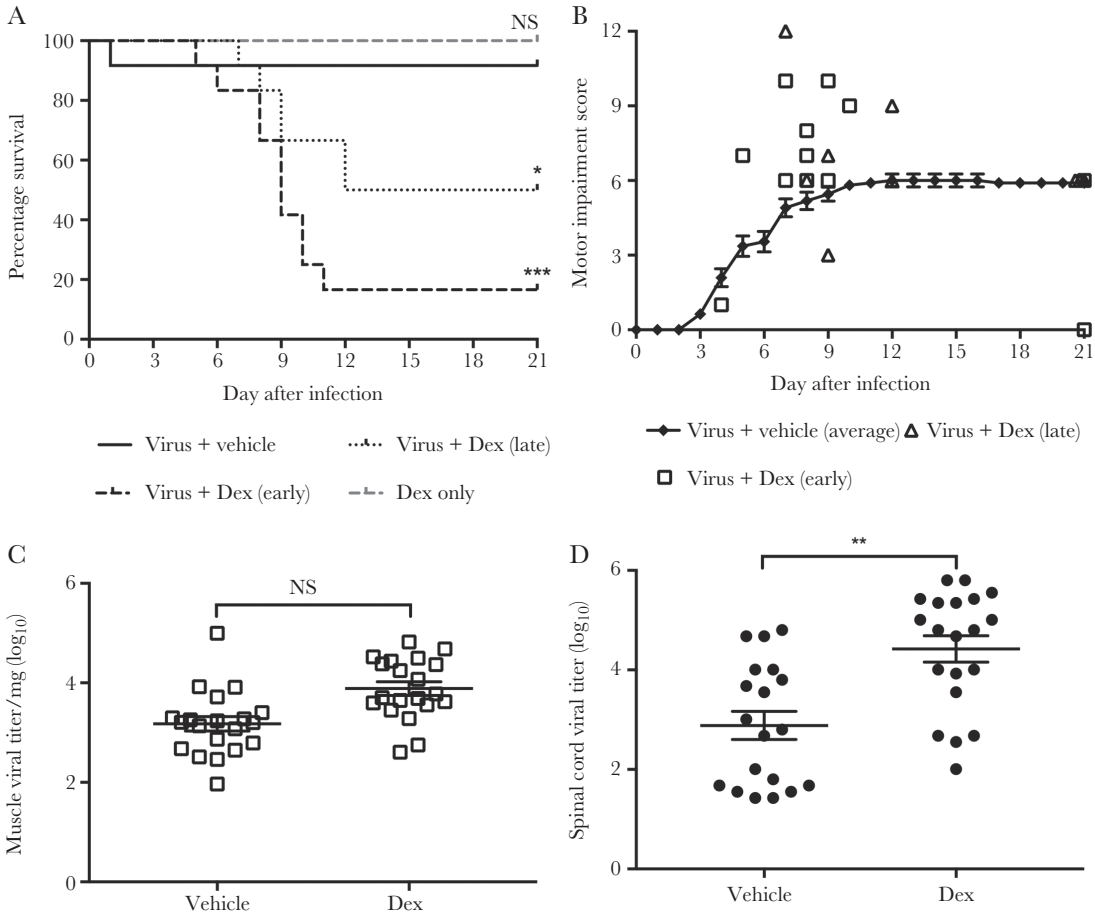

Figure 5. Dexamethasone (Dex) significantly worsens enterovirus D68 (EV-D68)–induced motor impairment and increases viral loads. *A,* Survival curves for mice given intraperitoneal Dex either 3 and 4 days (early treatment; n = 12) or 6 and 7 days (late treatment; n = 12) following intramuscular infection with 10^3 $TCID_{50}$ EV-D68 IL/14-18952 versus controls receiving virus with vehicle (solid black line; n = 12) or Dex only (dashed gray line; n = 21). *B,* Motor impairment scores of mice that died who received treatment with early (squares) and late (triangles) Dex treatment versus the average motor impairment score of surviving infected, vehicle treated controls (filled diamonds). *C* and *D,* Mice were given intramuscular 10^3 $TCID_{50}$ EV-D68 IL/14-18952 followed by Dex on days 3 and 4 after infection (n = 20) or vehicle (n = 20). On day 6 after infection, muscle (open squares) and spinal cord (filled circles) tissue specimens were collected from surviving mice for viral titer analysis. $^*P \le .05$, $^{**}P \le .01$, and $^{***}P \le .001$. NS, not significant.

ideal for identification of treatments that improve motor outcomes, as seen in a reduction of motor impairment scores, or of treatments that worsen motor impairment and produce higher mortality.

Patients with AFM from the 2014 US EV-D68 outbreak received hIVIG with little apparent improvement in symptoms [12, 16, 33]. However, before 2014, EV-D68 was rarely detected in the United States through routine enterovirus surveillance, suggesting that, before 2014, hIVIG lots may have had fewer anti–EV-D68 antibodies than current lots. Data from the current study suggest that recent lots of IVIG containing high levels of broadly neutralizing anti–EV-D68 antibodies could be affective at reducing the symptoms of EV-D68 CNS disease. The earlier after infection that mice received hIVIG, the better the motor outcome. Conversely, the benefits waned substantially as the disease progressed. These results suggest that hIVIG may be a reasonable empirical treatment for humans with EV-D68–associated AFM if the lots contain high titers of anti–EV-D68 antibody and therapy is given as early after onset of symptoms as possible.

Fluoxetine has been suggested as a potential treatment for AFM because of its antiviral effect against multiple EV-D68 strains in vitro, including EV-D68 IL/14-18952 [42]. Fluoxetine is an FDA-approved SSRI that has been shown to be safe and effective for the treatment of depression and anxiety in children and adults. The drug inhibits EV-D68 replication in cell culture through mechanisms independent of its action as an SSRI [36]. Fluoxetine has been used as part of combinatorial therapy in patients with EV-D68–associated AFM, but its efficacy, if any, is unknown [37, 38]. Although some pharmacokinetic and radioisotope MRI studies suggest that chronic fluoxetine treatment may result in CNS fluoxetine concentrations above the MIC for EV-D68, it is unclear whether these are achievable with acute

administration [42–44]. We found no beneficial effect of fluoxetine on improving motor outcomes in our EV-D68 paralysis model and no effect on reducing viral titers in muscle or spinal cord. Our model suggests no beneficial effect and possible harm (increased mortality in mice) in using fluoxetine, and this study does not support its continued use as empirical therapy.

Viral infections of the CNS can cause injury through direct infection of target cells. Infection also induces innate and acquired immune responses that can be beneficial in facilitating clearance of infection but can themselves contribute to immune-mediated cell and tissue injury. Intravenous steroids have been used in conjunction with antimicrobial agents to treat CNS infections in which inflammatory responses are believed to worsen tissue injury [45]. Evidence from the mouse model indicates that EV-D68–induced paralysis is cause by direct infection of motor neurons followed by motor neuron loss, rather than a delayed immune-mediated effect. In this model, treatment with the steroid dexamethasone resulted in increased viral load, worsening of motor impairment, and increased mortality. These data suggest that reducing the immune response during infection has a negative effect likely by inhibiting viral clearance and that the primary target of treatment should be the virus itself. This conclusion is also supported by the improvement of mice receiving hIVIG, which significantly decreased viral load in both the CNS and infected muscle tissue. Our results suggest that caution should be used in administering steroids as empirical therapy for EV-D68 AFM because they may worsen disease and increase mortality.

This study provides the first experimental evidence to help guide empirical therapy of EV-D68–associated AFM. These studies also establish the usefulness of the mouse model in screening other potential therapies, including antiviral drugs and other compounds that have shown in vitro efficacy against EV-D68 [35, 46].

Notes

Acknowledgments. We thank Dr Kevin Messacar and Amanda Hurst, PharmD, of Children's Hospital Colorado for providing guidance about the dosing and administration of fluoxetine and dexamethasone.

Financial support. This work was supported by the National Institutes of Health (grant R56 NS101208).

Potential conflicts of interest. All authors: No reported conflicts. All authors have submitted the ICMJE Form for Disclosure of Potential Conflicts of Interest. Conflicts that the editors consider relevant to the content of the manuscript have been disclosed.

References

1. Oberste MS, Maher K, Schnurr D, et al. Enterovirus 68 is associated with respiratory illness and shares biological features with both the enteroviruses and the rhinoviruses. J Gen Virol **2004**; 85:2577–84.
2. Blomqvist S, Savolainen C, Råman L, Roivainen M, Hovi T. Human rhinovirus 87 and enterovirus 68 represent a unique serotype with rhinovirus and enterovirus features. J Clin Microbiol **2002**; 40:4218–23.
3. Khetsuriani N, Lamonte-Fowlkes A, Oberst S, Pallansch MA; Centers for Disease Control and Prevention. Enterovirus surveillance—United States, 1970–2005. MMWR Surveill Summ **2006**; 55:1–20.
4. Schieble JH, Fox VL, Lennette EH. A probable new human picornavirus associated with respiratory diseases. Am J Epidemiol **1967**; 85:297–310.
5. Tokarz R, Firth C, Madhi SA, et al. Worldwide emergence of multiple clades of enterovirus 68. J Gen Virol **2012**; 93:1952–8.
6. Holm-Hansen CC, Midgley SE, Fischer TK. Global emergence of enterovirus D68: a systematic review. Lancet Infect Dis **2016**; 16:e64–75.
7. Messacar K, Abzug MJ, Dominguez SR. The emergence of enterovirus-D68. Microbiol Spectr **2016**; 4:105–19.
8. Aliabadi N, Messacar K, Pastula DM, et al. Enterovirus D68 infection in children with acute flaccid myelitis, Colorado, USA, 2014. Emerg Infect Dis **2016**; 22:1387–94.
9. Greninger AL, Naccache SN, Messacar K, et al. A novel outbreak enterovirus D68 strain associated with acute flaccid myelitis cases in the USA (2012-14): a retrospective cohort study. Lancet Infect Dis **2015**; 15:671–82.
10. Leshem E. Notes from the field: acute flaccid myelitis among persons aged </=21 years—United States, August 1-November 13, 2014. MMWR Morb Mortal Wkly Rep **2015**; 63:1243–4.
11. Messacar K, Abzug MJ, Dominguez SR. 2014 outbreak of enterovirus D68 in North America. J Med Virol **2016**; 88:739–45.
12. Messacar K, Schreiner TL, Van Haren K, et al. Acute flaccid myelitis: a clinical review of US cases 2012–2015. Ann Neurol **2016**; 80:326–38.
13. Midgley CM, Watson JT, Nix WA, et al. Severe respiratory illness associated with a nationwide outbreak of enterovirus D68 in the USA (2014): a descriptive epidemiological investigation. Lancet Respir Med **2015**; 3:879–87.
14. Millichap JG. Acute flaccid myelitis outbreak. Pediatr Neurol Briefs **2015**; 29:96.
15. Pastula DM, Aliabadi N, Haynes AK, et al.; Centers for Disease Control and Prevention (CDC). Acute neurologic illness of unknown etiology in children—Colorado, August–September 2014. MMWR Morb Mortal Wkly Rep **2014**; 63:901–2.
16. Sejvar JJ, Lopez AS, Cortese MM, et al. Acute flaccid myelitis in the United States, August–December 2014:

results of nationwide surveillance. Clin Infect Dis **2016**; 63:737–45.
17. Van Haren K, Ayscue P, Waubant E, et al. Acute flaccid myelitis of unknown etiology in California, 2012–2015. JAMA **2015**; 314:2663–71.
18. Centers for Disease Control and Prevention. Acute flaccid myelitis: AFM in the United States. http://www.cdc.gov/acute-flaccid-myelitis/afm-surveillance.html. Accessed 2 August 2017.
19. Maloney JA, Mirsky DM, Messacar K, Dominguez SR, Schreiner T, Stence NV. MRI findings in children with acute flaccid paralysis and cranial nerve dysfunction occurring during the 2014 enterovirus D68 outbreak. AJNR Am J Neuroradiol **2015**; 36:245–50.
20. Hovden IA, Pfeiffer HC. Electrodiagnostic findings in acute flaccid myelitis related to enterovirus D68. Muscle Nerve **2015**; 52:909–10.
21. Messacar K, Robinson CC, Pretty K, Yuan J, Dominguez SR. Surveillance for enterovirus D68 in colorado children reveals continued circulation. J Clin Virol **2017**; 92:39–41.
22. Wang G, Zhuge J, Huang W, et al. Enterovirus D68 subclade B3 strain circulating and causing an outbreak in the United States in 2016. Sci Rep **2017**; 7:1242.
23. Yoder JA, Lloyd M, Zabrocki L, Auten J. Pediatric acute flaccid paralysis: enterovirus D68–associated anterior myelitis. J Emerg Med **2017; 53:e19–e23.**
24. Antona D, Kossorotoff M, Schuffenecker I, et al. Severe paediatric conditions linked with EV-A71 and EV-D68, France, May to October 2016. Euro Surveill **2016**; 21:30402.
25. Cabrerizo M, García-Iñiguez JP, Munell F, et al. First cases of severe flaccid paralysis associated with enterovirus D68 infection in Spain, 2015–2016. Pediatr Infect Dis J **2017**. In press.
26. Carrion Martin AI, Pebody RG, Danis K, et al. The emergence of enterovirus D68 in England in autumn 2014 and the necessity for reinforcing enterovirus respiratory screening. Epidemiol Infect **2017**; 145:1855–64.
27. Crone M, Tellier R, Wei XC, et al. Polio-like illness associated with outbreak of upper respiratory tract infection in children. J Child Neurol **2016**; 31:409–14.
28. Dyrdak R, Grabbe M, Hammas B, et al. Outbreak of enterovirus D68 of the new B3 lineage in Stockholm, Sweden, August to September 2016. Euro Surveill **2016**; 21:pii: 30403.
29. Knoester M, Scholvinck EH, Poelman R, et al. Upsurge of enterovirus D68, the Netherlands, 2016. Emerg Infect Dis **2017**; 23:140–3.
30. Stacpoole SRL, Molyneux A, Bäumer D. Acute segmental poliomyelitis-like flaccid paralysis in an adult in the UK, associated with enterovirus D68. Pract Neurol **2017**; 17:297–301.
31. Yip CCY, Lo JYC, Sridhar S, et al. First report of a fatal case associated with EV-D68 infection in Hong Kong and emergence of an interclade recombinant in China revealed by genome analysis. Int J Mol Sci **2017**; 18:E1065.
32. Pérez G, Rosanova MT, Freire MC, et al. Unusual increase of cases of myelitis in a pediatric hospital in Argentina. Arch Argent Pediatr **2017**; 115:364–9.
33. Martin JA, Messacar K, Yang ML, et al. Outcomes of Colorado children with acute flaccid myelitis at 1 year. Neurology **2017**; 89:129–37.
34. Hixon AM, Yu G, Leser JS, et al. A mouse model of paralytic myelitis caused by enterovirus D68. PLoS Pathog **2017**; 13:e1006199.
35. Rhoden E, Zhang M, Nix WA, Oberste MS. In vitro efficacy of antiviral compounds against enterovirus D68. Antimicrob Agents Chemother **2015**; 59:7779–81.
36. Ulferts R, van der Linden L, Thibaut HJ, et al. Selective serotonin reuptake inhibitor fluoxetine inhibits replication of human enteroviruses B and D by targeting viral protein 2C. Antimicrob Agents Chemother **2013**; 57:1952–6.
37. Macaya A, Felipe-Rucián A. Enterovirus and neurological complications. An Pediatr (Barc) **2017**; 86:107–9.
38. Hurley D. After a lull last year, reports of acute flaccid myelitis surge in 2016. Neurology Today **2016**; 16:1, 21–3.
39. Goody RJ, Schittone SA, Tyler KL. Experimental reovirus-induced acute flaccid paralysis and spinal motor neuron cell death. J Neuropathol Exp Neurol **2008**; 67:231–9.
40. Zhang Y, Moore DD, Nix WA, Oberste MS, Weldon WC. Neutralization of enterovirus D68 isolated from the 2014 US outbreak by commercial intravenous immune globulin products. J Clin Virol **2015**; 69:172–5.
41. Gromeier M, Wimmer E. Mechanism of injury-provoked poliomyelitis. J Virol **1998**; 72:5056–60.
42. Tyler KL. Rationale for the evaluation of fluoxetine in the treatment of enterovirus D68-associated acute flaccid myelitis. JAMA Neurol **2015**; 72:493–4.
43. Strauss WL, Unis AS, Cowan C, Dawson G, Dager SR. Fluorine magnetic resonance spectroscopy measurement of brain fluvoxamine and fluoxetine in pediatric patients treated for pervasive developmental disorders. Am J Psychiatry **2002**; 159:755–60.
44. Wilens TE, Cohen L, Biederman J, et al. Fluoxetine pharmacokinetics in pediatric patients. J Clin Psychopharmacol **2002**; 22:568–75.
45. Fitch MT, van de Beek D. Drug Insight: steroids in CNS infectious diseases—new indications for an old therapy. Nat Clin Pract Neurol **2008**; 4:97–104.
46. Sun L, Meijer A, Froeyen M, et al. Antiviral activity of broad-spectrum and enterovirus-specific inhibitors against clinical isolates of enterovirus D68. Antimicrob Agents Chemother **2015**; 59:7782–5.